

A Complex Evolutionary History for the Disease Susceptibility *CDHR3* Locus

Mary B. O'Neill,^{1,2,3†*} Guillaume Laval,³ João C. Teixeira,^{3,4} Ann C. Palmenberg,⁵ Caitlin S. Pepperell^{2**}

¹Laboratory of Genetics, University of Wisconsin-Madison, Madison, WI 53706, USA

²Departments of Medicine and Medical Microbiology and Immunology, University of Wisconsin-Madison, Madison, WI 53706, USA

³Human Evolutionary Genetics Unit, CNRS UMR2000, Center of Bioinformatics, Biostatistics and Integrative Biology, Institut Pasteur, Paris 75015, France

⁴Australian Centre for Ancient DNA, The University of Adelaide, Adelaide, South Australia 5005, Australia

⁵Institute for Molecular Virology and Department of Biochemistry, University of Wisconsin—Madison, Madison, WI 53706, USA

† The majority of this work was carried out while MBO was a graduate student at the University of Wisconsin – Madison. Current affiliations are also listed.

* moneill@pasteur.fr

** cspepper@medicine.wisc.edu

1 **Abstract**

2 Selective pressures imposed by pathogens have varied among human populations throughout
3 their evolution, leading to marked inter-population differences at some genes mediating
4 susceptibility to infectious and immune-related diseases. A common polymorphism resulting in a
5 C₅₂₉ versus T₅₂₉ change in the Cadherin-Related Family Member 3 (*CDHR3*) receptor is
6 associated with rhinovirus-C (RV-C) susceptibility and severe childhood asthma. Given the
7 morbidity and mortality associated with RV-C dependent respiratory infections and asthma, we
8 hypothesized that the protective variant has been under selection in the human population.
9 Supporting this idea, a recent cross-species outbreak of RV-C among chimpanzees in Uganda,
10 which carry the ancestral ‘risk’ allele at this position, resulted in a mortality rate of 8.9%. Using
11 publicly available genomic data, we sought to determine the evolutionary history and role of
12 selection acting on this infectious disease susceptibility locus. The protective variant is the
13 derived allele and is found at high frequency worldwide, with the lowest relative frequency in
14 African populations and highest in East Asian populations. There is minimal population structure
15 among haplotypes, and we detect genomic signatures consistent with a rapid increase in
16 frequency of the protective allele across all human populations. However, given strong evidence
17 that the protective allele arose in anatomically modern humans prior to their migrations out of
18 Africa and that the allele has not fixed in any population, the patterns observed here are not
19 consistent with a classical selective sweep. We hypothesize that patterns may indicate frequency-
20 dependent selection worldwide. Irrespective of the mode of selection, our analyses show the
21 derived allele has been subject to selection in recent human evolution.

22

23 **Keywords**

24 Selection, rhinovirus-C, asthma, *CDHR3*, population genetics, evolution

25

26 **Introduction**

27 There is accumulating evidence to suggest that immunity-related genes are preferential targets of
28 natural selection (reviewed in ¹⁻⁵), supporting the notion that infectious diseases have been
29 important selective forces on human populations⁶. However, for most candidate loci, the
30 mechanisms and phenotypic effects underlying the observed signatures of selection remain
31 elusive.

32 Human rhinoviruses (RV) are found worldwide and are the predominant cause of the
33 common cold. While many RV infections cause only minor illness, type C strains of the virus are
34 associated with higher virulence. Unlike RV-A and RV-B, RV-C utilizes the Cadherin Related
35 Family Member 3 (CHDR3) receptor to gain entry into host cells. A missense variant in *CDHR3*
36 (rs6967330, C529T) results in a 10-fold difference in virus binding and replication *in vitro*⁷, and
37 experimental evidence points to varied cell surface expression between the two forms of the
38 receptor as a likely mechanism⁸. Adding clinical support that *CDHR3* functions as an RV-C
39 receptor, the ancestral allele at rs6967330 has been found to be associated with an increased risk
40 of respiratory tract illness by RV-C in two birth cohorts⁹. The allele is also associated with a
41 severe form of childhood asthma, in accordance with the known role of RV, particularly RV-C,
42 in triggering asthma exacerbations¹⁰. Taken together, these studies suggest that host genetics
43 mediate differing susceptibility to RV-C infection and asthma by affecting interactions between
44 the virus and its receptor (e.g. whether or not the protein is expressed on the cell surface and is
45 thus visible to the virus).

46 A recent outbreak of lethal respiratory illness among wild chimpanzees was attributed to
47 human RV-C crossing species boundaries. All members of the infected chimpanzee population
48 were invariant for the ancestral variant at the homologous position corresponding to the human
49 rs6967330 variant. The outbreak resulted in a staggering 8.9% mortality rate¹¹, and suggests that
50 RV-C infection can result in a high mortality rate in a susceptible population. As respiratory
51 infections, particularly prior to the availability of modern medical interventions, represent
52 significant threats to human health¹²⁻¹⁵, *CDHR3*, and in particular rs6967330, represent a
53 promising candidate target of natural selection. In the present study, we investigated the
54 evolutionary history of this locus for which there already exists strong experimental and clinical
55 data linking genotype with phenotypes that appear to modulate disease susceptibility.

56

57 **Results & Discussion**

58 **Long-term evolution of the *CDHR3* locus**

59 Examination of the locus in an alignment of 100 vertebrate genomes^{16,17} revealed that the
60 *CDHR3* locus is highly conserved, with homologs present in 85 species (Figure 1). Tyrosine is
61 the ancestrally encoded amino acid at the homologous position 529 in the human protein
62 sequence. There appears to have been a mutation leading to an A529T amino acid change

63 introduced in a common ancestor of opossums, Tasmanian devils, and wallabies that results in
64 the encoding of a phenylalanine at the homologous position. Numerous vertebrates (elephant,
65 horse, rabbit, pika, naked mole-rat, rat, mouse, golden hamster, Chinese hamster, prairie vole,
66 and lesser Egyptian jerboa) spread throughout the species tree also encode a different amino acid
67 (histidine) at this position. Whether these mutations are fixed in each of these species requires
68 further sequencing, and the effect of these nonsynonymous substitutions on protein expression
69 and function remain to be explored.

70 Providing further evidence that the locus has been evolutionary constrained, rs6967330
71 has a positive Genomic Evolutionary Rate Profiling (GERP) score of 4.39, signifying a deficit of
72 substitutions compared to neutral expectations. Values of the statistic calculated for bases within
73 *CDHR3* range from -12.2 to 6.08 (mean = -0.15, sd = 2.59) and from -12.3 to 6.17 chromosome-
74 wide (mean = -0.09, sd = 1.91)^{17,18}. The apparent conservation of this locus suggests it is
75 important for the function of *CDHR3* and thus makes it an interesting candidate of natural
76 selection.

77

78 **Population diversity patterns of the *CDHR3* locus**

79 Excluding *Homo sapiens*, sequencing data from the remaining extant species comprising all
80 hominids (great apes) are invariant at the position corresponding to rs6967330¹⁹. Genotyping of
81 an additional 41 chimpanzees whose community experienced a severe respiratory outbreak of
82 RV-C in 2013 revealed that all individuals were homozygous for the ancestral allele¹¹. In
83 examining hominin genomes, we find that Neanderthals and Denisovans carry the ancestral
84 allele, while ancient specimens of anatomically modern humans carry both the ancestral and
85 derived alleles. In low coverage sequencing data of *H. sapiens* estimated to have lived between
86 5000-8000 years ago (using sequencing reads from 45 aDNA samples for which we felt
87 confident making diploid genotype calls) we estimate the allele frequencies at rs6967330 to be
88 34.4% A (ancestral) and 65.5% G (derived) (Table S1)²⁰. Higher coverage aDNA extracted from
89 a 7,000 year old skeleton found in Germany and an 8,000 year old skeleton from the Loschbour
90 rock shelter in Luxembourg reveals heterozygotes at the locus²¹. Finally, a 45,000 year old early
91 *H. sapiens* from western Siberia is a homozygote for the derived allele²². Collectively, these data
92 suggest that the derived allele likely arose in the evolutionary branch leading to anatomically
93 modern humans, although population data for Neanderthals and Denisovans remains scarce.

94 The locus represents a shared polymorphism in contemporary worldwide populations.
95 Based on whole genome sequence data for 2504 individuals from 26 different populations²³, we
96 find that the derived ('protective') G allele is, on average, very common in East Asian
97 populations (EAS, 93.0%), followed by admixed American populations (AMR, 85.7%), South
98 Asian populations (SAS, 80.0%), and European populations (EUR, 79.2%). It is least common in
99 African populations (AFR, 73.5%), albeit also at high frequency. At the individual population
100 level, allele frequencies of the derived G allele range from 68.8% ("Mende in Sierra Leone",
101 MSL) to 95.3% ("Peruvians from Lima, Peru", PEL) (Figure 2).

102 We next investigated linkage disequilibrium (LD) patterns around *CDHR3* with
103 Haploview²⁴. A tight LD block was identified on chromosome 7 from 105,657,078-105,659,873,
104 with only moderate LD decay extending up to 105,680,022. Considering only biallelic SNPs
105 with a minor allele frequency (MAF) > 0.01, haplotypes within these blocks were identified with
106 the Pegas package in R^{25,26}. Relationships among haplotypes occurring at >1% were inferred
107 using network analysis (Figure 3). Eight haplotypes at frequency $\geq 1\%$ were identified from the
108 region of high LD, with the majority of individuals in all populations carrying the same
109 haplotype with the derived G allele ($n = 3848$); two less frequent haplotypes carrying the derived
110 allele are found in various geographic regions. The ancestral allele is found in the remaining five
111 haplotypes, which vary in their distributions across regions. Twenty-eight haplotypes were found
112 using the same criteria of a MAF > 0.01 and haplotype frequency of > 1% in the larger genomic
113 block containing moderate LD. Phylogenetic reconstruction of the resulting haplotypes in this
114 region resulted in a clear separation of those carrying the ancestral and derived alleles.
115 Unexpectedly, Chimp, Neanderthal and Denisovan haplotypes are closer to *H. sapiens* A-
116 haplotypes suggesting that natural selection shaped the haplotype pattern (Figure S1).

117

118 **World-wide Selection at the locus**

119 Given the morbidity and mortality associated with viral respiratory infections^{13,15} and
120 severe childhood asthma^{12,14} particularly prior to the availability of modern medical
121 interventions, we hypothesized that the frequency of the protective G allele (resulting in a
122 Cys₅₂₉) at rs6967330 might have increased more rapidly than under neutrality. We performed
123 genome-wide scans for selection in the 26 populations of the 1000 Genomes Project²³. To do so,
124 we used the integrated haplotype score (iHS)²⁷ and the number of segregating sites by length

125 (nS_L)²⁸, which are designed to capture rapid increases in frequency of selected variants and have
126 been applied in the context of detecting recent positive selection^{27,29,30}. We calculated these
127 neutrality statistics in each population independently and normalized by frequency-bin for all
128 loci with a DAF ≥ 0.2 (Figure S2). Fourteen populations presented extreme values of iHS and
129 nS_L ($\geq 95^{\text{th}}$ percentile of the distribution in the population) at rs6967330, with 2 and 5
130 populations falling in the 99th percentile for the two statistics, respectively. *CDHR3* lies in a
131 region of high recombination (1.8cM/Mb) and rs6967330 resides in a male specific
132 recombination hotspot^{17,31}. This may explain the slightly different patterns observed in nS_L and
133 iHS statistics, as an excess of extreme values of iHS have been observed at regions of low
134 recombination²⁸.

135 To investigate whether selection has acted on all populations simultaneously, we
136 implemented a multi-population (MP) combined statistic approach for iHS and nS_L . For each
137 SNP in each population, we combined the percent ranks of iHS and nS_L using Fisher's method,
138 and defined the MP-iHS and MP- nS_L as the resulting χ^2 value. We obtained a MP-iHS score of
139 156 and a MP- nS_L score of 157 for rs6967330. Both scores are in the 99th percentile, regardless
140 of whether we include only segregating sites in 2 or more populations or limit it to those SNPs
141 segregating in all 26 populations examined. This suggests that the derived allele at rs6967330 is
142 advantageous and that non-neutral processes have acted on this locus across global populations.

143

144 **A complex evolutionary scenario**

145 We originally hypothesized that selection pressures imposed by RV-C infection may have
146 resulted in a classic selective sweep at the locus; however, our results here are not consistent
147 with such a model. Preliminary dating estimates of RV-C point to a recent origin in the last few
148 thousand years⁸. We infer that the protective (derived) allele was already present in ancestral
149 populations at intermediate frequencies during this time frame (65.5% in aDNA dated 5,000-
150 8,000 years ago). Haplotype-based statistics such as iHS and nS_L have low power to detect
151 selection occurring on standing variation with intermediate frequency³². This suggests that
152 patterns of variation observed at rs6967330 are unlikely to have resulted from selection imposed
153 by RV-C itself; our findings suggest instead that an alternative selective agent(s) may have
154 been/be acting on the *CDHR3* locus prior to emergence of RV-C. These findings well parallel
155 those observed at the chemokine receptor gene-5 (*CCR-5*), where an unknown historical

156 selective pressure maintained a deletion in this gene that attenuates infectivity and disease
157 progression of HIV (reviewed in ³³), because that mutation clearly predates the emergence of
158 AIDS.

159

160 **Frequency-dependent Selection**

161 Several lines of evidence point to the derived allele at rs6967330 arising before the out-of-Africa
162 dispersal, including a lack of haplotype structure (Figure 3) and the presence of the allele at
163 homozygous state in aDNA from anatomically modern humans dating back to ~45,000 year
164 old²⁰⁻²². While we find signatures of selection at the locus, the protective variant has not fixed in
165 any of the contemporary populations examined (Figure 2), contrary to expectations for a strongly
166 positively selected variant that arose prior to human migrations out of Africa³⁴. We therefore
167 wondered if balancing selection could explain observed patterns of variation at the locus, as
168 balancing selection can maintain functional diversity over long periods of time through
169 frequency-dependent selection, heterozygote advantage, pleiotropy, and fluctuating selection³⁵.
170 Until recently, evidence for balancing selection in the human genome was limited to a few
171 classical cases such as the heterozygous advantage conferred by the *HbS* sickle cell mutation
172 against malaria^{36,37}, genes of the major histocompatibility complex/human leukocyte antigen
173 complex³⁸, and the ABO blood group³⁹. Balancing selection, however, has recently been
174 recognized as more prevalent than previously thought, particularly in shaping human immune
175 system phenotypes^{35,40,41}. To test whether the rs6967330 locus has been under long-term
176 balancing selection (i.e. selection occurring over at least hundreds of thousands of generations
177 ^{38,42,43}), we examined the distribution of β , a recently developed summary statistic designed to
178 detect clusters of alleles at similar frequencies, in 1000 Genomes Project data⁴⁴. β was similar
179 across all populations around the rs6967330 locus, and values were not indicative of long-term
180 balancing selection (Figure S3).

181 Balancing selection operating over shorter timescales clearly also plays a role in shaping
182 human diversity (e.g. *HbS* sickle cell mutation^{36,37}). Such a short-term balancing selection
183 scenario could explain the signals we detected with haplotype-based statistics, as genomic
184 signatures of short-term balancing selection are predicted to be indistinguishable from
185 incomplete sweeps of positive selection^{27,41}. In both of these scenarios, the selected allele
186 rapidly increases in frequency, with the allele eventually fixing under positive selection or

187 oscillating around a steady state in the case of balancing selection. As a reminder, haplotype-
188 based selection methods suggest that rs6967330 rose in frequency faster than under neutrality,
189 both at the global and the individual population level. Furthermore, population differentiation as
190 measured with F_{ST} at this locus is low relative to other SNPs with the same frequency (Figure
191 S4), a finding that is also consistent with short-term balancing selection across multiple
192 populations^{35,38,41}. Based on our observation that the derived variant at rs6967330 was present at
193 high frequencies in ancient human specimens and in the homozygous state in the case of a
194 45,000-year-old fossil, we posit that this allele may have started to increase in frequency in
195 ancestral populations before reaching its current equilibrium frequency independently in
196 worldwide populations. The derived allele ranges in frequency from 68.8-95.3% in modern
197 human populations, which is compatible with an equilibrium frequency being high. It is possible
198 that as the allele frequency of the derived mutation reaches high frequencies in a population,
199 circulation of the viruses exploiting CDHR3 (past and present) are affected, with attendant
200 impacts on the selective pressures they impose on human populations. Such a frequency-
201 dependent selection scenario seems more plausible than that of a heterozygote advantage given
202 that in Danish children with severe asthma, having even one copy of the risk variant was
203 associated with increased risk of exacerbation and hospitalization¹⁰. If there were another virus
204 that exploited this receptor in past human populations, we might assume that heterozygotes
205 would similarly not be conferred protection.

206 In conclusion, our analyses combined *a priori* knowledge of a genetic variant underlying
207 variable susceptibility to RV-C infections^{7,9,11} with population genetic analyses of whole genome
208 sequence data to investigate the evolutionary history of the locus in *CDHR3*. The conservation of
209 the protein, combined with its complex evolutionary history, exemplifies the biological
210 importance of *CDHR3*, which may or may not be ultimately relevant to its function as the
211 cellular surface receptor for RV-C. We detected a worldwide signature of selection at this locus,
212 but also found that patterns of variation do not conform to the classic selective sweep model.
213 Instead, we posit the possibility of frequency-dependent balancing selection operating at this
214 locus which warrants more investigation into genotypic and biochemical effects of the variant
215 (e.g. whether there is any phenotypic benefit to being heterozygous, trade-offs of different
216 genotypes, etc.). Irrespective of the mode of selection, our analyses show that the derived allele
217 has been advantageous and selected for in recent human evolution.

218

219 **Methods**

220 **Datasets.** *1000 Genomes Project*. Individual level phased sequencing data from the 1000

221 Genomes Project Phase 3 dataset were downloaded from

222 <ftp://ftp.1000genomes.ebi.ac.uk/vol1/ftp/release/20130502/>²³.

223

224 *Ancient H. sapiens*. BAM files for each of the 230 individuals included in the study by

225 Mathieson *et. Al.*²⁰ were downloaded and converted to MPILEUP format using samtools⁴⁵. Low

226 coverage sequencing data at asthma susceptibility loci were manually inspected for each

227 individuals for which at least one read had mapped to the site. Manual diploid genotyping calls

228 were made for aDNA samples for which we felt confident making diploid genotype calls (Table

229 S1).

230

231 *Neandertal and Denisovan*. Geotypes for the Vindija, Altai, and Denisovan genomes⁴⁶

232 generated using snpAD, an ancient DNA damage-aware genotyper, were downloaded from

233 <http://cdna.eva.mpg.de/neandertal/Vindija/VCF/>.

234

235 *Great Apes*. Genotypes of primates sequences were obtained from

236 <https://eichlerlab.gs.washington.edu/greatape/data/> and converted to the corresponding human

237 regions with the LiftOver software¹⁷.

238

239 **Haplotype Networks.** Indels and multi-allelic sites were filtered out with bcftools⁴⁵. Variants

240 having a Hardy-Weinberg equilibrium exact test p-value below 1×10^{-5} as calculated using the –

241 hwe midp function in PLINK1.9⁴⁷ in any of the 26 populations were removed from all

242 populations. The core haplotype surrounding rs6967330 was identified using biallelic markers

243 within 100kb of rs6967330 in Haploview²⁴ from all 26 populations in the 1000 Genomes Phase 3

244 release. A large haplotype block was defined on Chromosome 7 from 105,657,078 to

245 105,680,022, and a smaller haplotype of Chromosome 7 from 105,657,078 to 105,659,873.

246 Haplotypes within the defined haplotype blocks were extracted from biallelic markers with a

247 minor allele frequency (MAF) > 0.01 with the Pegas package^{25,26}. Haplotypes occurring at >1%

248 (at least 26 individuals) in the total 1000 Genomes Project dataset were constructed into

249 networks. Genotypes from two high quality Neanderthal genomes and a Denisovan genome were
250 similarly extracted and used in network analyses.

251
252 **Haplotype-Based Selection Scans.** We computed iHS and nS_L using the method implemented in
253 Selink, a software to detect selection using whole-genome datasets ([https://github.com/h-e-](https://github.com/h-e-g/selink)
254 [g/selink](https://github.com/h-e-g/selink)). As iHS and nS_L are sensitive to the inferred ancestral/derived state of an allele, we
255 computed these statistics only when the derived state was determined unambiguously³². Results
256 were normalized by derived allele frequency (DAF) bins (from 0 to 1, increments of
257 0.025)^{27,32}. We also minimized the false-positive discovery by excluding SNPs with a DAF
258 below 0.2, as the power to detect positive selection has been shown to be limited at such low
259 frequencies^{27,32}. For each statistic, we considered the percent rank at rs6967330 relative to the
260 genome-wide distribution in each population.

261
262 In order to test selection shared among populations, we combined iHS and nS_L into a single
263 multi-population (MP) combined selection score, MP- iHS and MP- nS_L . The rationale behind
264 these composite approaches⁴⁸⁻⁵⁰ is that neutrality statistics, though expected to be correlated
265 among populations under neutrality, are more strongly correlated for positively selected variants
266 than for neutral variants. Indeed, under global positive selection, iHS and nS_L tend to become
267 negative in all populations while false positives will only be negative in a few populations.
268 Consequently, candidates genuinely selected in several populations should harbor extreme values
269 for MP- iHS and MP- nS_L . For each SNP and each population, we determined the empirical p -
270 value of iHS and nS_L , i.e. the rank of each statistic in the genome-wide distribution divided by
271 the number of SNPs. We then used the `combine_pvalues` function implementation of Fisher's
272 method⁵¹ of the SciPy python package to compute MP- iHS and MP- nS_L for every SNP (passing
273 the criteria above to compute iHS and nS_L) found in at least two populations.

274
275 **β Test for Long-Term Balancing Selection.** β scores for each population in the 1000 Genomes
276 Project were obtained from <https://github.com/ksiewert/BetaScan>.

277
278 **Population Differentiation.** Global F_{ST} was calculated with Selink ([https://github.com/h-e-](https://github.com/h-e-g/selink)
279 [g/selink](https://github.com/h-e-g/selink)).

280

281 **Acknowledgements**

282 We wish to thank Andrew Kitchen for his advice on phylogenetic analyses and Lluís Quintana-
283 Murci for feedback on the manuscript.

284

285 **Author Contributions**

286 MBO, CSP, and ACP conceived the project. MBO, GL, and JCT performed the analyses. MBO
287 drafted the paper and made the figures. All authors provided critical feedback, reviewed, and
288 edited the manuscript.

289

290 **Competing interests**

291 The authors declare no competing interests.

References

1. Barreiro, L. B. & Quintana-Murci, L. From evolutionary genetics to human immunology: how selection shapes host defence genes. *Nat Rev Genet* **11**, 17–30 (2010).
2. Siddle, K. J. & Quintana-Murci, L. The Red Queen's long race: human adaptation to pathogen pressure. *Current Opinion in Genetics & Development* **29**, 31–38 (2014).
3. Karlsson, E. K., Kwiatkowski, D. P. & Sabeti, P. C. Natural selection and infectious disease in human populations. *Nat Rev Genet* **15**, 379–393 (2014).
4. Fumagalli, M. & Sironi, M. Human genome variability, natural selection and infectious diseases. *Current Opinion in Immunology* **30**, 9–16 (2014).
5. Quach, H. & Quintana-Murci, L. Living in an adaptive world: Genomic dissection of the genus Homo and its immune response. *Journal of Experimental Medicine* **214**, 877–894 (2017).
6. Fumagalli, M. *et al.* Signatures of Environmental Genetic Adaptation Pinpoint Pathogens as the Main Selective Pressure through Human Evolution. *PLOS Genetics* **7**, e1002355 (2011).
7. Bochkov, Y. A. *et al.* Cadherin-related family member 3, a childhood asthma susceptibility gene product, mediates rhinovirus C binding and replication. *PNAS* **112**, 5485–5490 (2015).
8. Palmenberg, A. C. Rhinovirus C, Asthma, and Cell Surface Expression of Virus Receptor, CDHR3. *J. Virol.* JVI.00072-17 (2017). doi:10.1128/JVI.00072-17
9. Bønnelykke, K. *et al.* Cadherin-related Family Member 3 Genetics and Rhinovirus C Respiratory Illnesses. *Am J Respir Crit Care Med* **197**, 589–594 (2017).
10. Bønnelykke, K. *et al.* A genome-wide association study identifies CDHR3 as a susceptibility locus for early childhood asthma with severe exacerbations. *Nat Genet* **46**, 51–55 (2014).
11. Scully, E. J. *et al.* Lethal Respiratory Disease Associated with Human Rhinovirus C in Wild Chimpanzees, Uganda, 2013. *Emerg Infect Dis* **24**, 267–274 (2018).
12. Gern, J. E. The ABCs of Rhinoviruses, Wheezing, and Asthma. *J. Virol.* **84**, 7418–7426 (2010).

13. Bryce, J., Boschi-Pinto, C., Shibuya, K. & Black, R. E. WHO estimates of the causes of death in children. *The Lancet* **365**, 1147–1152 (2005).
14. Busse, W. W., Lemanske, R. F. & Gern, J. E. The Role of Viral Respiratory Infections in Asthma and Asthma Exacerbations. *Lancet* **376**, 826–834 (2010).
15. Ferkol, T. & Schraufnagel, D. The Global Burden of Respiratory Disease. *Annals ATS* **11**, 404–406 (2014).
16. Karolchik, D. *et al.* The UCSC Table Browser data retrieval tool. *Nucleic Acids Res.* **32**, D493–496 (2004).
17. Rosenbloom, K. R. *et al.* The UCSC Genome Browser database: 2015 update. *Nucleic Acids Res* **43**, D670–D681 (2015).
18. Cooper, G. M. *et al.* Distribution and intensity of constraint in mammalian genomic sequence. *Genome Res.* **15**, 901–913 (2005).
19. Prado-Martinez, J. *et al.* Great ape genetic diversity and population history. *Nature* **499**, 471–475 (2013).
20. Mathieson, I. *et al.* Genome-wide patterns of selection in 230 ancient Eurasians. *Nature advance online publication*, (2015).
21. Lazaridis, I. *et al.* Ancient human genomes suggest three ancestral populations for present-day Europeans. *Nature* **513**, 409–413 (2014).
22. Fu, Q. *et al.* The genome sequence of a 45,000-year-old modern human from western Siberia. *Nature* **514**, 445–449 (2014).
23. The 1000 Genomes Project Consortium. A global reference for human genetic variation. *Nature* **526**, 68–74 (2015).
24. Barrett, J. C., Fry, B., Maller, J. & Daly, M. J. Haploview: analysis and visualization of LD and haplotype maps. *Bioinformatics* **21**, 263–265 (2005).

25. Paradis, E. pegas: an R package for population genetics with an integrated–modular approach. *Bioinformatics* **26**, 419–420 (2010).
26. R Development Core Team. *R: A Language and Environment for Statistical Computing*. (R Foundation for Statistical Computing).
27. Voight, B. F., Kudravalli, S., Wen, X. & Pritchard, J. K. A Map of Recent Positive Selection in the Human Genome. *PLoS Biol* **4**, e72 (2006).
28. Ferrer-Admetlla, A., Liang, M., Korneliussen, T. & Nielsen, R. On detecting incomplete soft or hard selective sweeps using haplotype structure. *Mol Biol Evol* msu077 (2014).
doi:10.1093/molbev/msu077
29. Sabeti, P. C. *et al.* Detecting recent positive selection in the human genome from haplotype structure. *Nature* **419**, 832–837 (2002).
30. Ferrari, S. L., Ahn-Luong, L., Garnero, P., Humphries, S. E. & Greenspan, S. L. Two Promoter Polymorphisms Regulating Interleukin-6 Gene Expression Are Associated with Circulating Levels of C-Reactive Protein and Markers of Bone Resorption in Postmenopausal Women. *J Clin Endocrinol Metab* **88**, 255–259 (2003).
31. Kong, A. *et al.* Fine-scale recombination rate differences between sexes, populations and individuals. *Nature* **467**, 1099–1103 (2010).
32. Fagny, M. *et al.* Exploring the Occurrence of Classic Selective Sweeps in Humans Using Whole-Genome Sequencing Data Sets. *Mol Biol Evol* **31**, 1850–1868 (2014).
33. Arenzana-Seisdedos, F. & Parmentier, M. Genetics of resistance to HIV infection: Role of co-receptors and co-receptor ligands. *Seminars in Immunology* **18**, 387–403 (2006).
34. Stephan, W. Signatures of positive selection: from selective sweeps at individual loci to subtle allele frequency changes in polygenic adaptation. *Molecular Ecology* **25**, 79–88 (2016).

35. Key, F. M., Teixeira, J. C., de Filippo, C. & Andrés, A. M. Advantageous diversity maintained by balancing selection in humans. *Current Opinion in Genetics & Development* **29**, 45–51 (2014).
36. Allison, A. C. Protection Afforded by Sickle-cell Trait Against Subtertian Malarial Infection. *Br Med J* **1**, 290–294 (1954).
37. Shriner, D. & Rotimi, C. N. Whole-Genome-Sequence-Based Haplotypes Reveal Single Origin of the Sickle Allele during the Holocene Wet Phase. *The American Journal of Human Genetics* **102**, 547–556 (2018).
38. Leffler, E. M. *et al.* Multiple Instances of Ancient Balancing Selection Shared Between Humans and Chimpanzees. *Science* **339**, 1578–1582 (2013).
39. Ségurel, L. *et al.* The ABO blood group is a trans-species polymorphism in primates. *PNAS* **109**, 18493–18498 (2012).
40. Ferrer-Admetlla, A. *et al.* Balancing Selection Is the Main Force Shaping the Evolution of Innate Immunity Genes. *The Journal of Immunology* **181**, 1315–1322 (2008).
41. Andrés, A. M. *et al.* Targets of Balancing Selection in the Human Genome. *Mol Biol Evol* **26**, 2755–2764 (2009).
42. Wiuf, C., Zhao, K., Innan, H. & Nordborg, M. The Probability and Chromosomal Extent of *trans*-specific Polymorphism. *Genetics* **168**, 2363–2372 (2004).
43. Teixeira, J. C. *et al.* Long-Term Balancing Selection in LAD1 Maintains a Missense Trans-Species Polymorphism in Humans, Chimpanzees, and Bonobos. *Mol Biol Evol* **32**, 1186–1196 (2015).
44. Siewert, K. M. & Voight, B. F. Detecting Long-Term Balancing Selection Using Allele Frequency Correlation. *Mol Biol Evol* **34**, 2996–3005 (2017).
45. Li, H. *et al.* The Sequence Alignment/Map format and SAMtools. *Bioinformatics* **25**, 2078–2079 (2009).

46. Prüfer, K. *et al.* A high-coverage Neandertal genome from Vindija Cave in Croatia. *Science* eao1887 (2017). doi:10.1126/science.aao1887
47. Purcell, S. *et al.* PLINK: a tool set for whole-genome association and population-based linkage analyses. *Am J Hum Genet* **81**, 559–75 (2007).
48. Deschamps, M. *et al.* Genomic Signatures of Selective Pressures and Introgression from Archaic Hominins at Human Innate Immunity Genes. *Am J Hum Genet* **98**, 5–21 (2016).
49. Grossman, S. R. *et al.* A Composite of Multiple Signals Distinguishes Causal Variants in Regions of Positive Selection. *Science* **327**, 883–886 (2010).
50. Grossman, S. R. *et al.* Identifying Recent Adaptations in Large-Scale Genomic Data. *Cell* **152**, 703–713 (2013).
51. Fisher, R. A. Statistical Methods for Research Workers. in *Breakthroughs in Statistics* 66–70 (Springer, New York, NY, 1992). doi:10.1007/978-1-4612-4380-9_6
52. Marcus, J. H. & Novembre, J. Visualizing the geography of genetic variants. *Bioinformatics* **33**, 594–595 (2017).

Figures

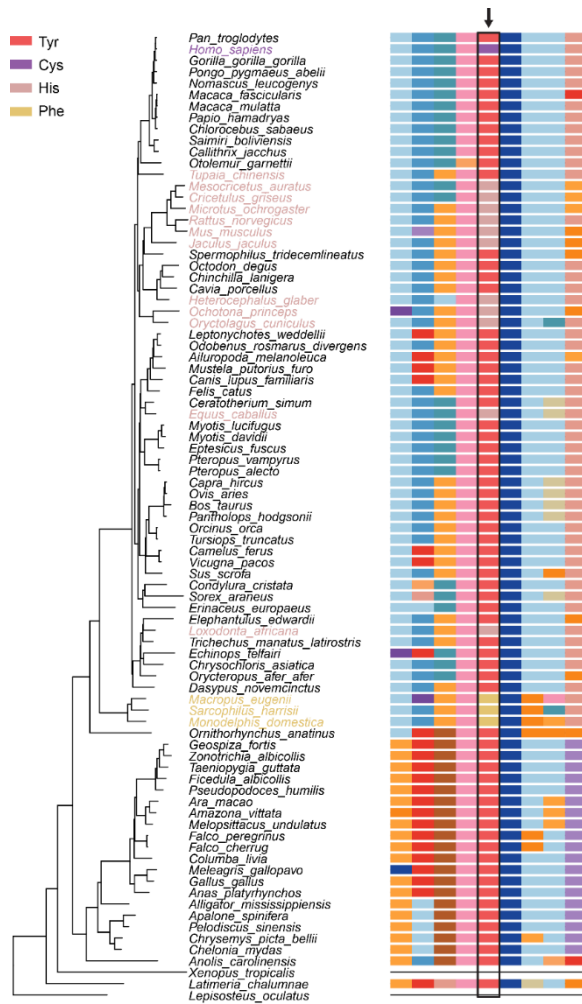


Figure 1. CDHR3 protein. (Left) Species tree for the multi sequence alignment of 85 species in the UCSC multiz alignment. (Right) Multi sequence protein alignment surrounding position 529 of the human CDHR3 protein. Residue 529 is outlined in black and designated with an arrow. Humans carry the Tyr and Cys alleles. Data obtained from the UCSC Genome Browser^{16,17}.

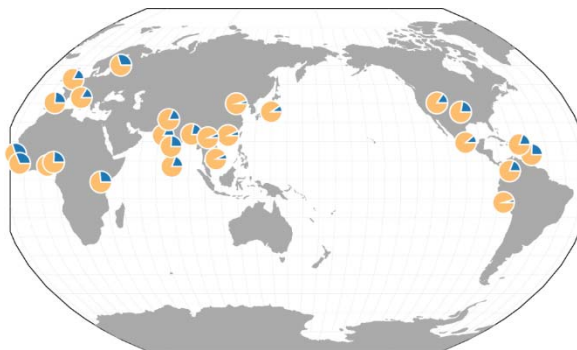


Figure 2. Global distribution of allele frequencies at rs6967330. Pie charts represent the relative allele frequencies of the ancestral A allele (blue) and the derived G allele (yellow) in each of the 26 populations of the 1000 Genomes Project²³. This image was generated through the *Geography of Genetic Variants* browser⁵².

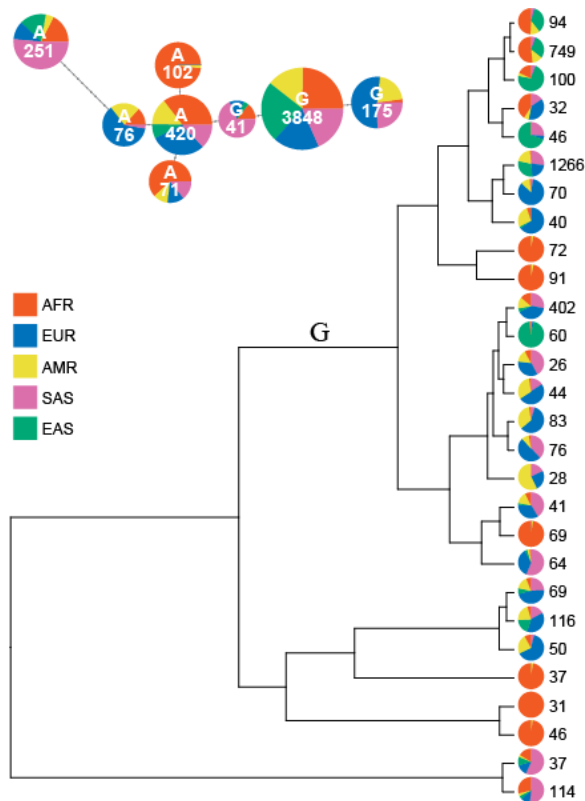


Figure 3. Haplotype structure of anatomically modern humans from the 1000 Genomes Project.

(Top) Haplotype network from chromosome 7 between 105,657,078 and 105,659,873. Haplotype network was constructed from phased genome sequences of 2504 individuals with variation at 16 sites in the 2,795bp region. Only haplotypes occurring at > 1% are shown. Colors reflect super population designation of individuals. (Bottom) Unrooted tree from chromosome 7 between 105,657,078 and 105,680,022. Haplotypes of the same 2504 individuals were derived for a larger haplotype block. Again, only haplotypes occurring at > 1% are shown and colors reflect super population designation of individuals. The tree is based on 83 SNPs (68 informative) from the 22,945bp region.